

---

# ENHANCING SAMPLE EFFICIENCY IN MULTI-AGENT RL WITH UNCERTAINTY QUANTIFICATION AND SELECTIVE EXPLORATION

---

**Tom Danino**

The Andrew and Erna Viterbi Faculty of  
Electrical & Computer Engineering  
Technion- Israel Institute of Technology  
tdanino12@gmail.com

**Nahum Shimkin**

The Andrew and Erna Viterbi Faculty of  
Electrical & Computer Engineering  
Technion- Israel Institute of Technology  
shimkin@ee.technion.ac.il

## ABSTRACT

Multi-agent reinforcement learning (MARL) methods have achieved state-of-the-art results on a range of multi-agent tasks. Yet, MARL algorithms typically require significantly more environment interactions than their single-agent counterparts to converge, a problem exacerbated by the difficulty in exploring over a large joint action space and the high variance intrinsic to MARL environments. To tackle these issues and enable sample-efficient learning, we propose a unified framework that extends multi-agent policy gradient (MAPG) with an ensemble of critics. Our key novelty lies in utilizing a diversity-regularized ensemble to perform selective exploration while efficiently reducing the variance inherent in the presence of multiple exploring agents. Specifically, we utilize ensemble disagreement, measured via excess kurtosis, to identify high-uncertainty states and actions for exploration. To reduce learning variance, we attenuate high-uncertainty samples via a novel uncertainty-aware variant of the TD( $\lambda$ ) algorithm, and compare its effectiveness to existing weighting methods. In addition to our main contribution, to maximize the utilization of training samples, we adapt the mixed actor approach for the underlying MAPG architecture. Such actors learn by mixing on-policy and off-policy losses, which allows for stable utilization of off-policy samples. The evaluation shows that our method outperforms state-of-the-art baselines on standard MARL benchmarks, including a variety of SMAC maps.

**Keywords** Multi-agent, Reinforcement learning, Ensemble learning, Selective exploration

## 1 Introduction

In recent years, *centralized training with decentralized execution* (CTDE) [1] has achieved state-of-the-art performance across challenging multi-agent benchmarks [2, 3, 4, 2]. CTDE enables parameter and information sharing during training while maintaining decentralized execution at test time. A key factor of its success is value decomposition, where a centralized mixing network decomposes a global value function into per-agent components, facilitating coordinated learning. This idea has also been extended to multi-agent policy gradient (MAPG) methods [5, 6], resulting in significant performance gains.

Despite this progress, CTDE methods remain vulnerable to the curse of dimensionality [7], as the joint action space grows exponentially with the number of agents and hinders effective exploration. This challenge is further exacerbated by the high variance common in MARL settings due to potentially suboptimal and exploratory behaviors of multiple agents [5]. Such conditions can lead to errors in the Bellman backup process and destabilize learning [8]. To address these challenges, we propose *SEMUS* (Sample-Efficient Multi-Agent Actor-Critic with Uncertainty Quantification and Selective Exploration), an ensemble-based MAPG framework designed to improve sample efficiency in large joint action spaces.

The primary component of SEMUS performs selective exploration while efficiently mitigating variance arising from multiple exploring agents. In our scheme, each agent maintains a (shared) ensemble of critics and leverages the *excess kurtosis* of the ensemble to identify high-uncertainty actions. We employ an ensemble approach (Fig. 1) since it has been demonstrated to be highly effective for uncertainty detection with good sample-efficiency properties. Rather than

relying on ensemble variance, as prior works from the single-agent RL suggest [8], we propose using ensemble kurtosis due to its higher sensitivity to outliers, which helps address efficiency in a large joint action space by reducing the amount of required exploration steps. While kurtosis has been used for uncertainty estimation in other domains [9, 10], to our knowledge, this is its first application for exploration in MARL. To reduce variance induced by multiple exploring agents, we introduce an uncertainty-based truncated TD( $\lambda$ ) critic, empirically outperforming Tree Backup (TB) in DOP [5]. Additionally, we limit ensemble overhead by promoting diversity among its members using Bhattacharyya regularization. This is motivated by prior works that show diversity prevents ensemble members from collapsing to similar solutions and enables smaller ensembles [11, 12]. A detailed ablation studies validating each component is provided in Sec. 7.

Finally, to maximize sample utilization, our underlying MAPG scheme extends the mixed actor approach [13] to MARL. By interpolating between on-policy and off-policy gradients, our actors leverage off-policy data while maintaining stability. Although off-policy learning improves sample efficiency, it introduces bias due to outdated samples, a problem amplified in multi-agent settings [13]. We mitigate this through controlled gradient mixing and provide an upper bound that shows the gradient bias depends on hyperparameters and the joint policy, which offers guidance for hyperparameter selection.

Our Contributions are as follows: (1) We introduce SEMUS, an ensemble-based MAPG algorithm that improves sample efficiency via kurtosis-driven selective exploration and uncertainty-aware TD( $\lambda$ ). (2) We propose Bhattacharyya regularization to promote ensemble diversity with minimal parameter overhead. (3) For the underlying MAPG algorithm, we adapt the mixed actor approach to MARL, enabling stable and efficient off-policy learning with bias analysis.

## 2 Background

**Decentralized partially observable Markov decision processes (Dec-POMDPs).** A Dec-POMDP models cooperative agents in a partially observable environment as the tuple  $\langle \mathcal{I}, \mathcal{S}, \mathcal{A}, \mathcal{P}, \Omega, \mathcal{O}, r, \gamma \rangle$ , where  $\mathcal{I}$  is a set of  $k$  agents and  $s \in \mathcal{S}$  the true state. Each agent selects  $a_i \in \mathcal{A}$ , forming the joint action  $\mathbf{a} = [a_i]_{i=1}^k \in \mathcal{A}$ , with shared reward  $r(s, \mathbf{a})$  and state transitions  $\mathcal{P}(s'|s, \mathbf{a})$ . Agents receive partial observations  $o_i \in \Omega$  via  $\mathcal{O}(o_i|s, a_i)$  and discount factor  $\gamma \in [0, 1)$ . Joint action-observation histories are  $\boldsymbol{\tau} \in \mathcal{T}$ , with policies  $\{\pi_{\theta_i}\}_{i=1}^k$ , behavior policies  $\{\mu_i\}_{i=1}^k$ , and actor logits  $\bar{z}^i = f_{\theta_i}(\boldsymbol{\tau}_i)$ .

**Value decomposition and monotonic constraints.** Value decomposition assigns credit to agents by splitting the global value into individual functions. The Individual-Global-Maximum (IGM) condition ensures that maximizing the global  $Q$  aligns with per-agent optima. the VDN (Value decomposition networks) approach sums individual  $Q$ -values, while QMIX [14] uses a centralized mixing network to represent  $Q_{\text{tot}}$  as a monotonic, non-linear combination.

**MAPG architecture and loss functions.** DOP [5] employs a centralized decomposed critic with decentralized actors. Its critic minimizes:

$$\mathcal{L}_{\text{critics}}(\phi) = \mathbf{c}\mathcal{L}^{\text{on-TD}(\lambda)}(\phi) + (1 - \mathbf{c})\mathcal{L}^{\text{off-TB}}(\phi), \quad (1)$$

balancing on-policy TD( $\lambda$ ) and off-policy tree backup (TB) updates, where  $\mathbf{c}$  is a tuning factor. The off-policy target is:

$$y^{\text{off}} = Q_{\text{tot}}^{\phi'}(\boldsymbol{\tau}, \mathbf{a}) + \sum_{t=0}^{m-1} \prod_{l=0}^t \left( \lambda \pi(\mathbf{a}_l | \boldsymbol{\tau}_l) \right) \left[ r_t + \gamma \mathbb{E}_{\mathbf{a}_{t+1} \sim \boldsymbol{\pi}} [Q_{\text{tot}}^{\phi'}(\boldsymbol{\tau}_{t+1}, \mathbf{a}_{t+1})] - Q_{\text{tot}}^{\phi'}(\boldsymbol{\tau}_t, \mathbf{a}_t) \right], \quad (2)$$

and the on-policy TD( $\lambda$ ) target is:

$$y^{\text{on}} = Q_{\text{tot}}^{\phi'}(\boldsymbol{\tau}, \mathbf{a}) + \sum_{t=0}^{\infty} (\gamma \lambda)^t [r_t + \gamma Q_{\text{tot}}^{\phi'}(\boldsymbol{\tau}_{t+1}, \mathbf{a}_{t+1}) - Q_{\text{tot}}^{\phi'}(\boldsymbol{\tau}_t, \mathbf{a}_t)]. \quad (3)$$

DOP's TB can unnecessarily truncate near-on-policy traces, reducing sample efficiency, a limitation we address in Sec. 4.

**Kurtosis.** The kurtosis of a random variable  $x$  is its fourth standardized moment [15] ( $\bar{x}$  denotes the sample mean):

$$\mathbb{E}\left[\left(\frac{x - \mu}{\sigma}\right)^4\right] = \frac{\mathbb{E}[(x - \mu)^4]}{(\mathbb{E}[(x - \mu)^2])^2}, \quad \kappa(\{x_i\}_{i=1}^N) = \frac{\frac{1}{N} \sum_{i=1}^N (x_i - \bar{x})^4}{\left[\frac{1}{N} \sum_{i=1}^N (x_i - \bar{x})^2\right]^2}, \quad (4)$$

$\kappa_{e, Q_i}^{\phi_i}$  is the excess kurtosis:

$$\kappa_{e, Q_i}^{\phi_i}(\boldsymbol{\tau}_i, a_i) = \kappa(\{Q^{\phi_i, j}(\boldsymbol{\tau}_i, a_i)\}_{j=1}^N) - 3. \quad (5)$$

For the  $i$ -th critic ensemble, raw kurtosis is (used for uncertainty weighting, Sec. 4):

$$\kappa_{Q_i}^{\phi_i}(\tau_i, a_i) = \kappa(\{Q^{\phi_{i,j}}(\tau_i, a_i)\}_{j=1}^N). \quad (6)$$

**Variance in multi-agent RL.** Variance measures reward fluctuations and can destabilize learning. In MARL, variance is amplified due to other agents’ exploratory or suboptimal behaviors [16]. In CTDE,  $\text{Var}[Q_{\text{tot}}]$  propagates through the centralized critic, e.g., for  $Q_{\text{tot}}^{\phi}(\tau, \mathbf{a}) = \sum_i \lambda_i(\tau)Q_i^{\phi_i}(\tau_i, a_i)$ , each agent’s updates are influenced by others’ variance via  $Q_{\text{tot}}$ .

### 3 Related Work

SEMUS builds on three main line of works: CTDE with MAPG and value decomposition, selective exploration in MARL, and ensemble learning with uncertainty estimation.

**MAPG and value decomposition.** PAC [6] and DOP [5] use a centralized decomposed critic with decentralized actors. DOP trains the critic with TD( $\lambda$ ) and per-agent Q-functions, employing on-policy actors. PAC uses a shared critic with off-policy actors and entropy regularization. SEMUS unifies these paradigms via mixed on-policy/off-policy actor losses, balancing bias and efficiency. We also improve critic efficiency by replacing DOP’s tree-backup (TB) coefficient with an uncertainty-aware coefficient. RISKQ [17] applies distributional RL with a risk-averse VaR criterion. Similar to SEMUS, it downweights high-uncertainty actions. We compare the two approaches on risk-based settings proposed by the RISKQ authors in the evaluation section.

**Selective exploration in MARL.** PAC [6] uses shared entropy with decaying temperature. ADER [18] applies adaptive entropy regularization for states needing more exploration. FOX [19] uses mutual information (MI) to guide meaningful state visitation. DJBD [4] learns a Lipschitz-constrained representation to encourage diverse trajectories. SEMUS differs by leveraging ensemble kurtosis for uncertainty-driven exploration, avoiding redundant exploration unlike entropy- or MI-based methods.

**Ensemble learning and uncertainty.** Ensembles improve exploration and sample efficiency in both single- and multi-agent RL. EMAX [20] combines ensembles with value decomposition and uses voting for action selection. UCB [21] uses ensemble variance as an exploration bonus in single-agent RL, and SUNRISE [8] extends this with combined exploration and uncertainty weighting. SEMUS differs by introducing novel exploration and weighting mechanisms that improve sample efficiency while maintaining small parameter overhead, and a novel ensemble diversity technique, replacing the simpler random initialization. Differences are further detailed in the discussion.

## 4 The SEMUS Algorithm

We present SEMUS, a unified algorithm designed to enhance sample efficiency and enable selective exploration. The main components are: (i) selective exploration via ensemble kurtosis (Sec. 4.2), (ii) uncertainty-weighted critic loss (Sec. 4.3), (iii) ensemble diversity via Bhattacharyya regularization (Sec. 4.4).

The complementary mechanism for the actor’s loss is presented in Sec. 5. Pseudocode is provided in Algorithms 1–2 (Appendix A).

### 4.1 Ensemble of critics

In our scheme, each individual critic  $i$  is composed of an ensemble of  $N$  sub-critics:

$$Q_i^{\phi_i}(\tau, a_i) = \frac{1}{N} \sum_{j=1}^N Q^{\phi_{i,j}}(\tau_i, a_i). \quad (7)$$

The mean  $Q$ -value of the  $i$ th agent is denoted by  $Q_i^{\phi_i}$ , while each member in the ensemble is denoted by  $Q^{\phi_{i,j}}$ . The global  $Q$ -function is decomposed into a linear combination of individual functions, as proposed by several previous works [5]:

$$Q_{\text{tot}}^{\phi}(\tau, \mathbf{a}) = \sum_{i=1}^K \lambda_i(\tau)Q_i^{\phi_i}(\tau_i, a_i) + b(\tau), \quad (8)$$

where  $K$  denotes the number of agents. To maintain the monotonic constraint, as suggested by QMIX, the mixing network coefficients  $\lambda_i$  are restricted to be positive.  $Q_{\text{tot}}$  also includes a learnable bias, denoted by  $b$  (see Fig. 1).

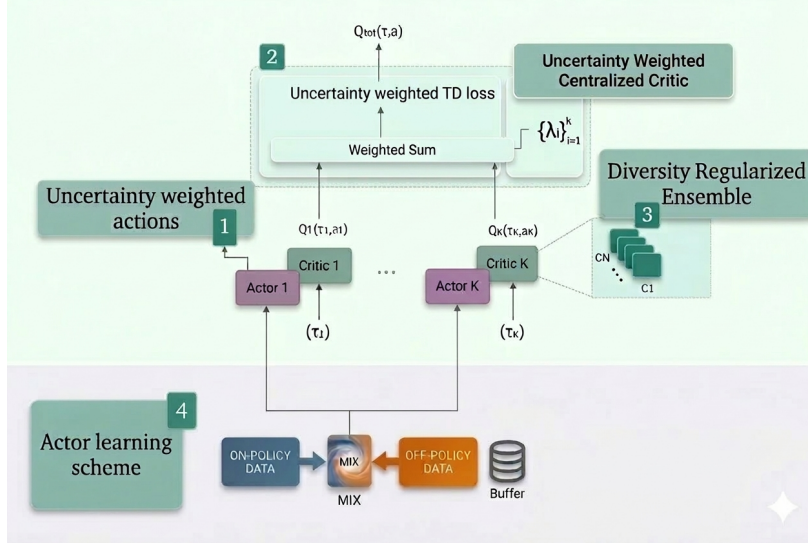


Figure 1: SEMUS architecture

## 4.2 Exploration based on ensemble kurtosis

Standard exploration techniques from single-agent RL, such as entropy maximization [22], can lead to inefficient exploration in MARL due to the large joint action space, often degrading performance [18]. These methods encourage random exploration [23], causing agents to visit redundant states [19]. To reduce exploration steps, we propose a selective approach: only high-uncertainty states and actions are explored. We leverage ensemble kurtosis to prioritize actions with higher kurtosis values, corresponding to greater disagreement in the ensemble. Kurtosis effectively captures the "tailness" of a distribution [15], emphasizing values deviating from the mean Q-function more than variance. This allows ignoring low-disagreement states, resulting in more efficient exploration. Sec. 7 empirically analyzes the ability of kurtosis to guide exploration to informative states

Our algorithm applies kurtosis in two ways. First, each agent detects high-uncertainty states based on the mean kurtosis across all actions. Second, in detected states, actions are weighted by their kurtosis. At each iteration, the  $i$ -th agent computes the kurtosis over its  $M_i$  actions:

$$\bar{g}_i(\tau_i, \{Q^{\phi_i, j}\}_{j=1}^{M_i}) = \frac{\sum_{z=1}^{M_i} \kappa_{e, Q_i}^{\phi_i}(\tau_i, a_z)}{M_i}, \quad (9)$$

where  $\kappa_{e, Q_i}^{\phi_i}$  is the excess kurtosis described in Eq. 5. If  $\bar{g}_i > 0$  then an exploration step is performed by adding the kurtosis of each action to the corresponding logits, otherwise, a standard action selection is executed. Conditioning on the positivity of  $\bar{g}_i$  guarantees exploration is performed only on areas of positive excess kurtosis. Formally, given the  $M_i$  logits of actor  $i$  on a given state, denoted by  $\bar{z}^i = \{z_1^i, \dots, z_{M_i}^i\}$ , and the corresponded ensemble excess kurtosis, denoted by  $\{\kappa_{e, Q_i}^{\phi_i}(\tau_i, a_1), \dots, \kappa_{e, Q_i}^{\phi_i}(\tau_i, a_{M_i})\}$ , then the  $j$ th weighted logit of actor  $i$  is given by:

$$\tilde{z}_j^i = \begin{cases} z_j^i + \beta \kappa_{e, Q_i}^{\phi_i}(\tau_i, a_j), & \text{if } \bar{g}_i > 0 \\ z_j^i, & \text{otherwise} \end{cases} \quad (10)$$

where  $\beta$  is a hyperparameter. The softmax operator is applied to the weighted logits.

## 4.3 Uncertainty weighted decomposed critic

We suggest incorporating attenuation based on uncertainty into the loss function for efficient variance reduction. Reducing variance via ensemble uncertainty weighting is highly effective in single-agent RL [8]; we propose a novel variation of this approach to account for the presence of multiple exploring agents while also maintaining higher sample efficiency.

At the first step, we quantify uncertainty for each agent by employing the kurtosis of the ensemble. To obtain a bounded score, we adopt the weight function proposed by [8]:

$$w_i(\tau_i, a_i) = 0.5 + \mathcal{S}(-C_1 \kappa_{e, Q_i}^{\phi_i}(\tau_i, a_i)), \quad (11)$$

	TB ( $C_{\tau}^{\text{dop}}$ )	SEMUS ( $C_{\tau}$ )
SMAC (IS ratio)	$0.25 \pm 0.17$	$0.81 \pm 0.16$
PP (IS ratio)	$0.21 \pm 0.15$	$0.80 \pm 0.05$

Table 1: Performance (IS ratio)

	GPU memory	Single-pass latency
Single critic (N=1)	0.59MB	0.0015[s]
Ensemble (N=5)	2.95MB	0.0024[s]
Ensemble (N=10)	5.9MB	0.00349[s]

Table 2: Computational complexity

where  $\kappa_{Q_i}^{\phi_i}$  is defined in Eq. 6. Notice that differently from the exploration phase, we use the raw kurtosis rather than the excesses, which ensures the term is always positive such that  $\frac{1}{2} \leq w_i(\tau_i, a_i) \leq 1$ .  $\mathcal{S} : \mathbb{R} \rightarrow (0, 1)$  denotes the sigmoid function and  $C_1$  is a scaling factor. Note that  $\kappa_{Q_i}^{\phi_i}$  was originally calculated as ensemble variance; as our initial experiments showed kurtosis yielded better results, we substituted the variance term.

The weighted uncertainty of the entire team of agents is denoted by:

$$w(\boldsymbol{\tau}, \mathbf{a}) = \frac{\sum_{i=1}^k \lambda_i(\boldsymbol{\tau}) w_i(\tau_i, a_i)}{\sum_{i=1}^k \lambda_i(\boldsymbol{\tau})}. \quad (12)$$

Given  $w(\boldsymbol{\tau}, \mathbf{a})$ , we can construct the critic loss. Our architecture is built on DOP [5], which showed TD( $\lambda$ ) to be highly effective in CTDE settings. Similar to DOP, we train the centralized critic by combining off-policy and on-policy loss functions:

$$\mathcal{L}_{\text{critics}}(\phi) = \mathbf{c} \mathcal{L}^{\text{on}}(\phi) + (1 - \mathbf{c}) \mathcal{L}^{\text{off}}(\phi), \quad (13)$$

where  $\mathbf{c}$  is the relative scaling factor, used to balance between off-policy and on-policy updates. To construct the loss function, we use off-policy samples for  $\mathcal{L}^{\text{off}}$  (from replay buffer), while  $\mathcal{L}^{\text{on}}$  is calculated with on-policy samples. The novelty in our critic, compared to DOP, stems from the change in  $\mathcal{L}^{\text{off}}$ . First, we apply the standard off-policy loss:

$$y^{\text{off}} = Q_{\text{tot}}^{\phi'}(\boldsymbol{\tau}, \mathbf{a}) + \sum_{t=0}^{m-1} (\gamma \lambda)^t C_{\tau} [r_t + \gamma \mathbb{E}_{\mathbf{a}_{t+1} \sim \pi} [Q_{\text{tot}}^{\phi'}(\boldsymbol{\tau}_{t+1}, \mathbf{a}_{t+1})] - Q_{\text{tot}}^{\phi'}(\boldsymbol{\tau}_t, \mathbf{a}_t)], \quad (14)$$

but rather than using the lower efficiency  $C_{\tau}^{\text{dop}} = \prod_{l=0}^t \lambda \pi(\mathbf{a}_l | \boldsymbol{\tau}_l)$  TB coefficient, suggested by [24], we replace it with our uncertainty-based coefficient.

To construct our coefficient, we employ the retrace coefficient:  $\min(1, \frac{\pi(\mathbf{a} | \boldsymbol{\tau})}{\mu(\mathbf{a} | \boldsymbol{\tau})})$ , but instead of truncation to 1 we propose truncation based on the uncertainty score, which quantifies how much the ensemble of critics is uncertain about the chosen joint action, i.e.,  $C_{\tau} = \prod_{l=0}^t \min(w(\boldsymbol{\tau}_l, \mathbf{a}_l), \frac{\pi(\mathbf{a}_l | \boldsymbol{\tau}_l)}{\mu(\mathbf{a}_l | \boldsymbol{\tau}_l)})$ . This yields full utilization to 1 only when there is no uncertainty, allowing the learning algorithm to assign lower coefficient values when the current policy is less trustworthy. In Table 1, we analyze sample efficiency (based on IS-ratio measurements) of both approaches, comparing SEMUS with  $C_{\tau}^{\text{dop}}$  to SEMUS with the clipped uncertainty-based ratio  $C_{\tau}$ . Ablation is provided in Fig. 3. The overall off-policy loss is calculated as  $\mathcal{L}^{\text{off}}(\phi) = \mathbb{E}_{\beta} [(y^{\text{off}} - Q_{\text{tot}}^{\phi}(\boldsymbol{\tau}, \mathbf{a}))^2]$ . The on-policy loss is calculated similarly to DOP (Eq. 3).

Note that the multiplicative approach is similar to traditional techniques [24], which multiply the coefficients up to the current time  $t$ . Also, since  $w$  is bounded, it can be seen as a subtraction of an uncertainty threshold  $\epsilon$ , subtracted from 1, i.e.,  $w(\boldsymbol{\tau}_l, \mathbf{a}_l) = 1 - \epsilon$ .

#### 4.4 Ensemble diversity via Bhattacharyya regularization

Previous works from the single-agent domain showed that encouraging diversity in an ensemble can dramatically reduce the required size of the ensemble. To this end, we propose utilizing the Bhattacharyya distance as a regularization term. Bhattacharyya distance is widely used in classification and clustering tasks due to its ability to measure distributional overlap [25]. It is known to maintain reliable results when different samples differ from one another, even in the near orthogonal case [26]. This property aligns with our goal, as we are maximizing diversity and attempting to make the samples as different as possible. To our knowledge, there have been no prior efforts to apply the Bhattacharyya distance in the context of ensemble diversity, despite studies indicating it to be highly stable for measuring similarity [27]. The Bhattacharyya term is calculated as the sum of distances between the mean  $Q$ -function of the ensemble  $Q_i^{\phi_i}$  and all the distinct  $Q$ -functions:

$$\delta_{B_{\text{total}}}^{Q_i}(\tau_i) = \sum_{j=1}^N -\ln \left( \sum_{a \in \mathcal{A}} \sqrt{\sigma(Q_i^{\phi_i}(\tau_i, a)) \sigma(Q_i^{\phi_i, j}(\tau_i, a))} \right), \quad (15)$$

The regularization term is added to the critic’s loss ( $C_2$  is analyzed in Table ??):

$$\mathcal{L}_{\text{total}}(\phi) = \mathcal{L}_{\text{critics}}(\phi) - C_2 \sum_{i=1}^K \delta_{B_{\text{total}}}^{Q_i}(\tau_i). \quad (16)$$

## 5 Actor Training Scheme – mixed on-policy and off-policy

The actor’s loss serves as a complementary component to the SEMUS algorithm. We examine 3 different options: on-policy, off-policy, and mixed actor. Comparison between the three approaches is given in Sec. 7. While previous MAPG and value decomposition approaches either trained the actors in an on-policy [5] or off-policy manner [6], we suggest improving existing schemes by interpolating both losses, which improves training samples utilization but with lower bias compared to strict off-policy. Specifically, we adapt the interpolated loss function [13] to MARL by accounting for  $Q_{\text{tot}}$  and the mixing network. In our scheme, each actor trains by combining gradients from on and off loss functions [13]:

$$D_{\nu}^{\beta}(\pi_i, \pi_{-i}) = (1 - \nu) \mathbb{E}_{\rho^{\pi, \pi_i}} [\nabla_{\theta_i} \log \pi_i(a_i | \tau_i; \theta_i) U_{\pi_i}^{\phi_i}(\tau_i, a_i)] \\ + \nu \mathbb{E}_{\rho^{\beta}} [\nabla_{\theta_i} \bar{Q}_{\text{tot}}^{\phi}(\tau, (a_i, \mathbf{a}_{-i}))], \quad (17)$$

where  $\bar{Q}_{\text{tot}}^{\phi}(\tau, (a_i, \mathbf{a}_{-i})) = \mathbb{E}_{\pi_i} [Q_{\text{tot}}^{\phi}(\tau, (a_i, \mathbf{a}_{-i}))]$ , and  $\nu$  is the relative scaling factor. The joint off-policy is denoted by  $\beta(\mathbf{a} | \tau) = \prod_{i=1}^k \beta_i(a_i, \tau_i)$ , and  $\rho^{\beta}$  is the joint off-policy state distribution.  $U_i$  is the advantage function [5]:

$$U_i^{\phi_i}(\tau_i, a_i) = \lambda_i(\tau) (Q_i^{\phi_i}(\tau_i, a_i) - \sum_{x \in \mathcal{A}} \pi_{\theta_i}(x | \tau_i) Q_i^{\phi_i}(\tau_i, x)). \quad (18)$$

Combining both approaches is known to produce good results [13] in single-agent RL with higher stability compared to off-policy training. Sec. 6, shows that the bias in our gradient updates remains bounded under proper  $\nu$  configurations.

## 6 Bounds on Bias and Additional Analysis

This section presents the following results: (1) A bound on the bias of mixed actor updates, (2) Bhattacharyya as lower bound on pairwise diversity. (3) Analysis of kurtosis vs variance for (epistemic) uncertainty detection.

**Bias of mixed on-and-off policy actor updates.** This section presents the following results: (1) A bound on the bias of mixed actor updates, (2) Bhattacharyya as lower bound on pairwise diversity. (3) Analysis of kurtosis vs variance for (epistemic) uncertainty detection.

**Bias of mixed on-and-off policy actor updates.** Since each agent independently updates its policy, we analyze the bias on a per-agent basis. Let the true Q-function be [5]:

$$Q_i^{\pi}(\tau, a_i) = \sum_{\mathbf{a}_{-i}} \pi_{-i}(\mathbf{a}_{-i} | \tau_{-i}) Q_{\text{tot}}^{\pi}(\tau, (a_i, \mathbf{a}_{-i})), \quad (19)$$

with gradient:

$$\nabla_{\theta_i} J(\pi_i, \pi_{-i}) = \mathbb{E}_{\tau \sim \rho^{\pi}, a_i \sim \pi_i} [\nabla_{\theta_i} \log \pi_i(a_i | \tau_i) Q_i^{\pi}(\tau, a_i)]. \quad (20)$$

The approximation error is  $Q_{\phi_i}^{\pi}(\tau, a_i) = Q_i^{\pi}(\tau, a_i) - \lambda_i(\tau) Q_i^{\phi_i}(\tau_i, a_i)$ . The bias of the mixed gradient  $D_{\nu}^{\beta}$  is bounded as follows:

**Proposition 1.** Let  $D_{\text{max}}^{\text{KL}}(\pi, \beta) = \max_{\tau} D_{\text{KL}}(\pi(\cdot | \tau), \beta(\cdot | \tau))$ , and define:

$$\omega_1 = \max_{\tau, \mathbf{a}} \|\nabla_{\theta_i} \log \pi_i(a_i | \tau_i) \lambda_i(\tau) Q_{\phi_i}^{\pi}(\tau, a_i)\|_1, \\ \omega_2 = \max_{\tau} \|\nabla_{\theta_i} \lambda_i(\tau) \mathbb{E}_{\pi_i} [Q_i^{\phi_i}(\tau_i, a_i)]\|_1. \quad (21)$$

Then:

$$\|\nabla_{\theta_i} J(\pi_i, \pi_{-i}) - D_{\nu}^{\beta}(\pi_i, \pi_{-i})\|_1 \leq \frac{\omega_1}{1 - \gamma} + \frac{2\omega_2\nu\gamma}{(1 - \gamma)^2} \sqrt{D_{\text{max}}^{\text{KL}}(\pi, \beta)}. \quad (22)$$

The proof is given in D. The bound shows that the bias in each agent’s gradient update is driven by two factors: (i) the approximation error of  $Q_i^{\pi}$ , captured by  $Q_{\phi_i}^{\pi}$ , and (ii) the divergence between the joint on-policy distribution and the behavior policy used to collect off-policy data.

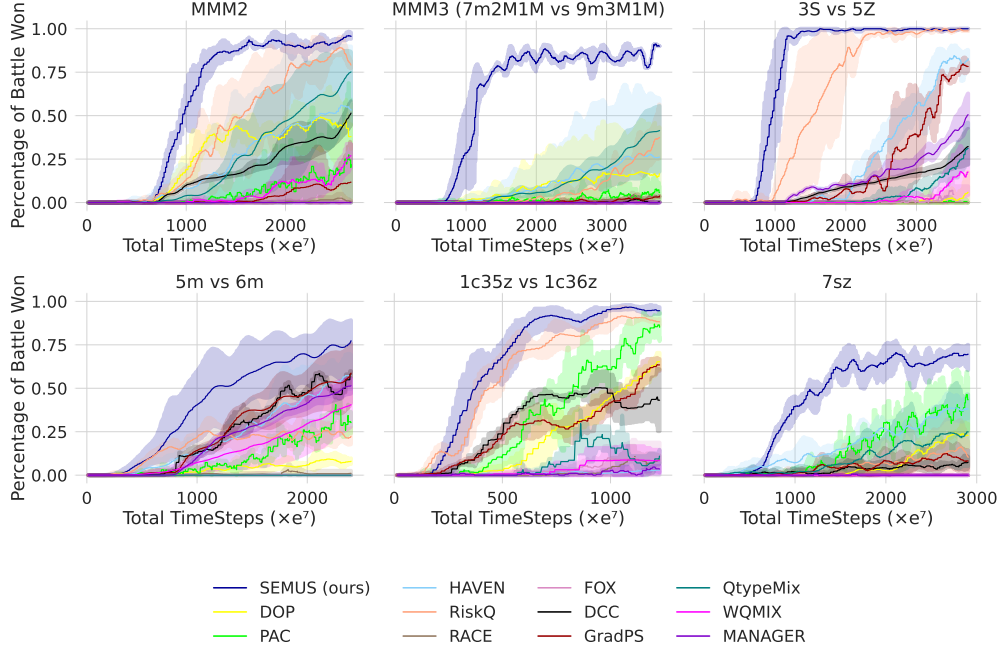


Figure 2: Results on the SMAC benchmark

**Bounds on the Bhattacharyya distance.** We show that using the mean Q-function to regularize the ensemble provides a lower bound on the stronger pairwise diversity, which is often treated as an upper bound in entropy-based methods[28]. This approach reduces computation from  $\mathcal{O}(N^2)$  of the pairwise to  $\mathcal{O}(N)$ . The proof is given in E.

**Proposition 2.** Let the pairwise Bhattacharyya distance between all pairs be defined as:

$$\delta_{\text{pairwise}}^i = \frac{1}{N^2} \sum_{j_1=1}^N \sum_{j_2=1}^N \delta_B(\sigma(Q^{\phi_{i,j_1}}(\tau_i, \cdot)), \sigma(Q^{\phi_{i,j_2}}(\tau_i, \cdot))), \quad (23)$$

and the mean Bhattacharyya distance between the mean and each member be denoted by  $\delta_{\text{mean}}^i = \frac{\delta_{B_{\text{total}}}^{Q_i}(\tau_i)}{N}$ . Then the following holds:

$$\delta_{\text{mean}}^i \leq \delta_{\text{pairwise}}^i. \quad (24)$$

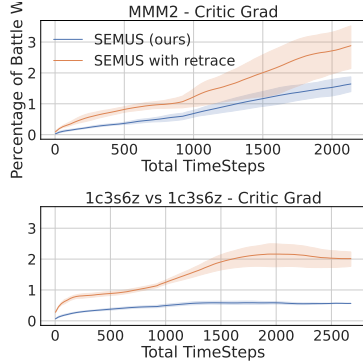
**Kurtosis vs variance.** The normalization in kurtosis reduces sensitivity to the magnitude of deviations [29]. This is a desired property when our goal is to detect when critics disagree, rather than how extreme their predictions are. Specifically, this can improve stability during exploration while still reliably detecting high uncertainty action. To further illustrate the robustness of kurtosis to disagreement magnitudes, consider a simplified model where the critics' estimates satisfy (for given state and action)  $Q^{\phi_{i,j}} = \mu + \delta_j$ ,  $j = 1, \dots, N$ , where  $\delta_j \in \{0, \Delta\}$  denotes a possible epistemic shift of constant magnitude from the normal value  $\mu$ . Let  $\delta_j = \Delta$  with probability  $p_j$  and  $\delta_j = 0$  otherwise, and denote  $\bar{p} = \frac{1}{N} \sum_j p_j$ . Here, while the ensemble variance is clearly proportional to  $\Delta^2$ , kurtosis depends only on the disagreement probability  $\bar{p}$  and not on the magnitude  $\Delta$  (see Lemma 1 below, and its proof in Appendix F).

**Lemma 1.** For every  $\Delta > 0$ ,  $\text{Var}[\{Q^{\phi_{i,j}}\}_{j=1}^N] = \bar{p}(1-\bar{p})\Delta^2$ , whereas  $\kappa(\{Q^{\phi_{i,j}}\}_{j=1}^N) = \frac{1-6\bar{p}(1-\bar{p})}{\bar{p}(1-\bar{p})}$ .

## 7 Experiments and Results

We evaluate SEMUS across standard MARL benchmarks: SMAC [30], multi-agent car following (MACF) [17], and predator-prey (PP) [6]. Hyperparameters and network architectures are fixed across experiments (Appendix B). Each experiment uses six seeds with 95% confidence intervals. SEMUS is compared to DCC [31], QtypeMix [32], GradPS [2], weighted QMIX [1], DOP [5], FOX [19], HAVEN [33], PAC [6], RiskQ [17], MANAGER [3], and RACE [34]. The ensemble size is  $N = 10$ . Each critic implemented as a 2-layer FC network.

**Performance on SMAC.** Figure 2 shows SEMUS consistently outperforms baselines across six SMAC maps. The advantage is pronounced on super-hard maps MMM2 and MMM3, where diversity among agents is critical. RiskQ and



	TB (DOP)	SEMUS (retrace)	SEMUS (uncertainty)
MMM2	$0.79 \pm 0.052$	$0.85 \pm 0.06$	<b><math>0.94 \pm 0.042</math></b>
MACF (reward)	$-112 \pm 9$	$-129 \pm 12$	<b><math>-82 \pm 19</math></b>
1c35z vs 1c36z	$0.7 \pm 0.04$	$0.87 \pm 0.04$	<b><math>0.96 \pm 0.003</math></b>

Figure 3: Component analysis – critic coefficient

Table 3: Ablation analysis – actors, exploration, and diversity

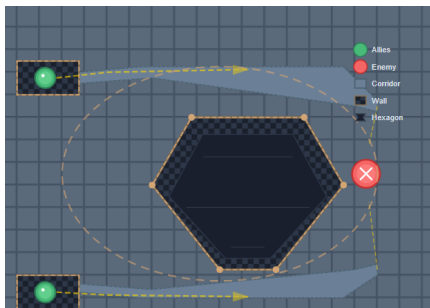
	Original	On-policy	Off-policy	Exploration ( $\beta = 0$ )	Diversity ( $C_2 = 0$ )
MMM2	<b><math>0.94 \pm 0.042</math></b>	$0.65 \pm 0.02$	$0.83 \pm 0.05$	$0.77 \pm 0.04$	$0.74 \pm 0.05$
MMM3	<b><math>0.82 \pm 0.03</math></b>	$0.6 \pm 0.07$	$0.71 \pm 0.02$	$0.66 \pm 0.03$	$0.69 \pm 0.052$
1c35z vs 1c36z	<b><math>0.96 \pm 0.003</math></b>	$0.92 \pm 0.01$	$0.87 \pm 0.03$	$0.79 \pm 0.01$	$0.85 \pm 0.045$

QtypeMix, which handle heterogeneous agents, rank second and third. DOP performs well only on MMM maps, likely due to stochasticity from softmax policies enhancing diversity.

**Two corridors and predator-prey.** To demonstrate effective exploration, we evaluate SEMUS on the two-corridors map [35] and PP. In the two-corridors task, agents can traverse either a short or long corridor, but the short corridor is closed mid-training, requiring adaptation. SEMUS adapts significantly faster, achieving the best performance (results in Fig. 5, map in Fig. 4). We further show that excess kurtosis guides agents toward informative states (Fig. 4). Specifically, we measure the agents’ utilization of the long corridor from convergence until the short corridor is closed. Higher long-corridor usage reflects more diverse behavior compared to consistently taking the short path, which enables much faster adaptation once the corridor closes (0.1M steps versus 4M without guided exploration). In PP (Fig. 5), we construct settings with an increasingly larger grid, where 4 agents have to be involved in every catch. This makes catching prey and rewards much more sparse than in the default settings. Both HAVEN, which incorporates intrinsic reward, and SEMUS achieved good results in PP, specifically in the larger grid, where state exploration is required.

**MACF.** Here, two agents, each controlling a car, need to reach a goal collaboratively while staying in each other’s sight. The aim is to reach the goal as fast as possible, but if any of the cars overspeed, it crashes with some probability (inducing uncertainty). SEMUS achieves higher rewards (Fig. 5) while minimizing overspeed events (Table 5). This shows the performance improvement corresponds to agents learning to avoid overspeed, or in the case of SEMUS, down-weighting of high uncertainty actions. We use this setting to verify the effectiveness of our uncertainty weighting when aleatoric noise is present in the environment.

**Parameter analysis.** Table ?? presents a detailed analysis of  $\beta$ ,  $C_1$ ,  $C_2$ ,  $N$ , and  $\nu$ . Smaller values of  $\nu$  (below 0.5)



	With kurtosis	Without kurtosis
% long corridor	44%	23%
Adaptation time (steps)	0.1M	0.4M

Figure 4: Percentage of time the long corridor is used in the 2 corridor map, and time required to adapt once the short corridor is closed.

	$\nu=0.3$	$\nu = 0.5$ (original)	$\nu=0.6$
MMM2	$0.89 \pm 0.1$	<b><math>0.93 \pm 0.04</math></b>	$0.84 \pm 0.1$
MMM3	$0.65 \pm 0.02$	<b><math>0.82 \pm 0.01</math></b>	$0.73 \pm 0.02$
1c35z vs 1c36z	<b><math>0.962 \pm 0.01</math></b>	$0.96 \pm 0.003$	$0.89 \pm 0.07$

(a) Parameter analysis ( $\nu$ )

	$C_1 = 0.25$	$C_1 = 0.5$ (original)	$C_1 = 0.75$
MMM2	$0.91 \pm 0.06$	<b><math>0.93 \pm 0.04</math></b>	$0.84 \pm 0.06$
MMM3	<b><math>0.84 \pm 0.05</math></b>	$0.82 \pm 0.01$	$0.76 \pm 0.01$
MACF	$-109 \pm 22$	$-85 \pm 18$	<b><math>-79 \pm 8</math></b>

(b) Parameter analysis ( $C_1$ )

	N=5	N=10 (original)	N=15
MMM2	$0.87 \pm 0.05$	<b><math>0.93 \pm 0.04</math></b>	$0.9 \pm 0.05$
MMM3	$0.72 \pm 0.015$	$0.82 \pm 0.01$	<b><math>0.84 \pm 0.017</math></b>
1c35z vs 1c36z	$0.91 \pm 0.03$	<b><math>0.96 \pm 0.003</math></b>	$0.87 \pm 0.08$

(c) Parameter analysis (N)

	$\beta=0.001$	$\beta=0.004$ (original)	$\beta=0.01$
MMM2	$0.79 \pm 0.05$	<b><math>0.93 \pm 0.04</math></b>	$0.78 \pm 0.04$
MMM3	$0.66 \pm 0.015$	<b><math>0.82 \pm 0.01</math></b>	$0.6 \pm 0.06$
Sparse PP	$15 \pm 2.1$	$17.5 \pm 2.4$	<b><math>18.4 \pm 1.3</math></b>

(d) Parameter analysis ( $\beta$ )

	$C_2 = 0.0001$	$C_2 = 0.002$ (original)	$C_2 = 0.01$
MMM2	$0.85 \pm 0.07$	<b><math>0.93 \pm 0.04</math></b>	$0.81 \pm 0.06$
MMM3	$0.76 \pm 0.01$	<b><math>0.82 \pm 0.01</math></b>	$0.71 \pm 0.01$
MACF	$-90 \pm 22$	$-82 \pm 19$	<b><math>-74 \pm 10.1</math></b>

(e) Parameter analysis ( $C_2$ )

sometimes outperform  $\nu = 0.5$ , likely due to reduced bias from approximation errors or inter-agent interactions, suggesting that  $\nu$  should be kept at or below 0.5. Higher  $C_1$  increases uncertainty weights, which can reduce training data utilization in most SMAC maps, but improves performance in MACF by avoiding risky high-uncertainty states. For  $\beta$ , increased exploration generally hinders performance, although in exploration-heavy environments like Sparse PP, higher  $\beta$  can be beneficial.

**Component ablations.** We evaluate the contributions of SEMUS components through ablation studies: (1) Disabling Bhattacharyya regularization ( $C_2 = 0$  in Table 3) and comparing it to Theil index [12] (Table 6a), second, no exploration ( $\beta = 0$ ) is reported in Table 3. (2) Actor loss: Comparing on-policy, off-policy, and mixed training (Table 3) shows that mixed actors consistently perform best, with off-policy second and on-policy last. (3) Critic loss: Our truncated TD( $\lambda$ ) improves sample utilization and win rates over the original TB and retrace (Table 1, Fig. 3). The variance reduction effect of SEMUS is also depicted in Fig. 3. (4) Kurtosis vs Variance and raw kurtosis for exploration (Table 6a).

### Discussion.

**Computation requirements analysis.** We use an ensemble of size  $N = 10$ , with diversity regularization helping maintain performance with a relatively small ensemble [11, 12]. As all critic share the same ensemble (standard approach in cooperative MARL) and assuming each critic network has  $P$  parameters, the overhead in terms of memory is  $O(NP)$  for the entire system. Table 2 shows time and parameter measurements on GPU.

**Comparison to ensemble-based approaches.** Ensemble methods have been effective for simultaneous exploration and down-weighting of high-variability samples in single-agent RL [8]. Our approach differs from the SAC ensemble of [8] in several ways. First, SEMUS uses a single actor that adjusts its action distribution via a lightweight critic-only ensemble, reducing parameter overhead compared to their heavier ensembles of both actors and critics. Exploration is guided by an excess-kurtosis signal rather than variance, preventing excessive exploration and improving training

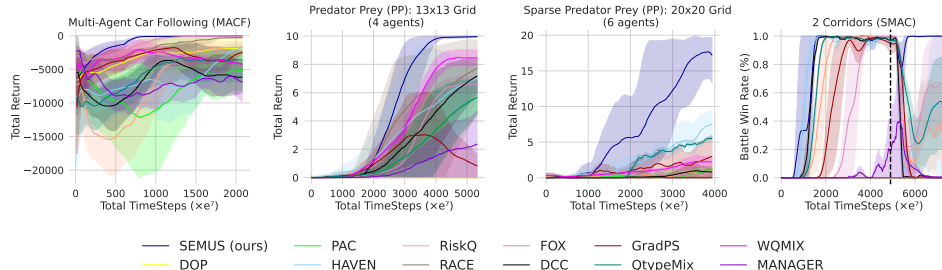


Figure 5: Results on predator-prey, MACF, and 2 corridors map (SMAC)

Table 5: MACF - number of over-speeds over training

	$t=30(\times e^7)$	$t=250^*(\times e^7)$	$t=500(\times e^7)$
SEMUS	$132 \pm 43$	$19 \pm 37$	$0.3 \pm 0.6$
RACE	$238 \pm 36$	$93 \pm 61$	$80 \pm 95$
RISKQ	$290 \pm 152$	$253 \pm 71$	$136 \pm 96$

efficiency (Tables 3, 6a). Second, instead of simply weighting Bellman targets by uncertainty, we introduce a  $TD(\lambda)$  variant that improves sample utilization while down-weighting high-uncertainty samples. Third, we employ a novel ensemble diversity method, beyond random initialization and varied training samples, to further enhance learning.

## 8 Conclusion

We present SEMUS, a novel MARL algorithm that combines MAPG architectures with ensemble techniques to improve sample efficiency in high-dimensional MARL settings. SEMUS introduces selective exploration guided by ensemble excess kurtosis, and variance reduction via an uncertainty-weighted  $TD(\lambda)$  critic. Ensemble overhead is minimized using Bhattacharyya-based diversity, and mixed actor updates maximize training sample utilization, improving both stability and efficiency. Our results demonstrate that simultaneous exploration and variance reduction are feasible even under high epistemic and aleatoric uncertainty induced by multiple agents. Evaluation shows that SEMUS achieves SOTA performance on known benchmarks including super hard SMAC maps.

## References

- [1] Tabish Rashid, Gregory Farquhar, Bei Peng, and Shimon Whiteson. Weighted qmix: Expanding monotonic value function factorisation for deep multi-agent reinforcement learning. *Advances in neural information processing systems*, 33:10199–10210, 2020.
- [2] Haoyuan Qin, Zhengzhu Liu, Chenxing Lin, Chennan Ma, Songzhu Mei, Siqi Shen, and Cheng Wang. GradPS: Resolving futile neurons in parameter sharing network for multi-agent reinforcement learning. In *Forty-second International Conference on Machine Learning*, 2025.
- [3] Yangkun Chen, Kai Yang, Jian Tao, and Jiafei Lyu. Novelty-guided data reuse for efficient and diversified multi-agent reinforcement learning. In *Proceedings of the AAAI Conference on Artificial Intelligence*, volume 39, pages 15930–15938, 2025.
- [4] Tianxu Li and Kun Zhu. Learning joint behaviors with large variations. In *Proceedings of the AAAI Conference on Artificial Intelligence*, volume 39, pages 23249–23257, 2025.
- [5] Yihan Wang, Beining Han, Tonghan Wang, Heng Dong, and Chongjie Zhang. DOP: Off-policy multi-agent decomposed policy gradients. In *International conference on learning representations*, 2020.
- [6] Hanhan Zhou, Tian Lan, and Vaneet Aggarwal. PAC: Assisted value factorization with counterfactual predictions in multi-agent reinforcement learning. *Advances in Neural Information Processing Systems*, 35:15757–15769, 2022.
- [7] Wei Du and Shifei Ding. A survey on multi-agent deep reinforcement learning: from the perspective of challenges and applications. *Artificial Intelligence Review*, 54(5):3215–3238, 2021.

	Original	Variance-based exploration	Raw Kurtosis exploration	Theil index
1c35z vs 1c36z	<b>0.96 ± 0.003</b>	0.63 ± 0.062	0.88 ± 0.02	0.84 ± 0.04
MMM2	<b>0.94 ± 0.042</b>	0.67 ± 0.08	0.83 ± 0.052	0.8 ± 0.04
MMM3	<b>0.82 ± 0.03</b>	0.64 ± 0.039	0.79 ± 0.05	0.71 ± 0.03

(a) Components analysis – exploration and diversity (Theil index)

- [8] Kimin Lee, Michael Laskin, Aravind Srinivas, and Pieter Abbeel. SUNRISE: A simple unified framework for ensemble learning in deep reinforcement learning. In *International Conference on Machine Learning*, pages 6131–6141. PMLR, 2021.
- [9] IP Zakharov and OA Botsyura. Calculation of expanded uncertainty in measurements using the kurtosis method when implementing a bayesian approach. *Measurement techniques*, 62:327–331, 2019.
- [10] Wenxin Dai, Zhenling Mo, Chong Luo, Jing Jiang, and Qiang Miao. Bearing fault diagnosis based on reinforcement learning and kurtosis. In *2019 Prognostics and System Health Management Conference (PHM-Qingdao)*, pages 1–5. IEEE, 2019.
- [11] Chao Li, Chen Gong, Qiang He, and Xinwen Hou. Keep various trajectories: Promoting exploration of ensemble policies in continuous control. *Advances in Neural Information Processing Systems*, 36, 2024.
- [12] Hassam Sheikh, Mariano Phielipp, and Ladislau Boloni. Maximizing ensemble diversity in deep reinforcement learning. In *International Conference on Learning Representations*, 2021.
- [13] Shixiang Shane Gu, Timothy Lillicrap, Richard E Turner, Zoubin Ghahramani, Bernhard Schölkopf, and Sergey Levine. Interpolated policy gradient: Merging on-policy and off-policy gradient estimation for deep reinforcement learning. *Advances in neural information processing systems*, 30, 2017.
- [14] Tabish Rashid, Mikayel Samvelyan, Christian Schroeder De Witt, Gregory Farquhar, Jakob Foerster, and Shimon Whiteson. Monotonic value function factorisation for deep multi-agent reinforcement learning. *The Journal of Machine Learning Research*, 21(1):7234–7284, 2020.
- [15] Peter H Westfall. Kurtosis as peakedness, 1905–2014. rip. *The American Statistician*, 68(3):191–195, 2014.
- [16] Jakub Grudzien Kuba, Muning Wen, Linghui Meng, Haifeng Zhang, David Mguni, Jun Wang, Yaodong Yang, et al. Settling the variance of multi-agent policy gradients. *Advances in Neural Information Processing Systems*, 34:13458–13470, 2021.
- [17] Siqi Shen, Chennan Ma, Chao Li, Weiquan Liu, Yongquan Fu, Songzhu Mei, Xinwang Liu, and Cheng Wang. RISKQ: risk-sensitive multi-agent reinforcement learning value factorization. *Advances in Neural Information Processing Systems*, 36:34791–34825, 2023.
- [18] Woojun Kim and Youngchul Sung. An adaptive entropy-regularization framework for multi-agent reinforcement learning. In *International Conference on Machine Learning*, pages 16829–16852. PMLR, 2023.
- [19] Yonghyeon Jo, Sunwoo Lee, Junghyuk Yeom, and Seungyul Han. FOX: Formation-aware exploration in multi-agent reinforcement learning. In *Proceedings of the AAAI Conference on Artificial Intelligence*, volume 38, pages 12985–12994, 2024.
- [20] Lukas Schäfer, Oliver Slumbers, Stephen McAleer, Yali Du, Stefano V. Albrecht, and David Mguni. Ensemble value functions for efficient exploration in multi-agent reinforcement learning. *AAMAS ’25*, page 1849–1857, Richland, SC, 2025. International Foundation for Autonomous Agents and Multiagent Systems.
- [21] Richard Y Chen, Szymon Sidor, Pieter Abbeel, and John Schulman. UCB exploration via q-ensembles. *arXiv preprint arXiv:1706.01502*, 2017.
- [22] Tuomas Haarnoja, Aurick Zhou, Pieter Abbeel, and Sergey Levine. Soft actor-critic: Off-policy maximum entropy deep reinforcement learning with a stochastic actor. In *International conference on machine learning*, pages 1861–1870. PMLR, 2018.
- [23] Benjamin Eysenbach and Sergey Levine. Maximum entropy RL (provably) solves some robust RL problems. In *International Conference on Learning Representations*, 2022.
- [24] Rémi Munos, Tom Stepleton, Anna Harutyunyan, and Marc Bellemare. Safe and efficient off-policy reinforcement learning. *Advances in neural information processing systems*, 29, 2016.
- [25] Michal Pándy, Andrea Agostinelli, Jasper Uijlings, Vittorio Ferrari, and Thomas Mensink. Transferability estimation using bhattacharyya class separability. In *Proceedings of the IEEE/CVF Conference on Computer Vision and Pattern Recognition*, pages 9172–9182, 2022.

- [26] Rahul Ramesh, Jialin Mao, Itay Griniasty, Rubing Yang, Han Kheng Teoh, Mark Transtrum, James P Sethna, and Pratik Chaudhari. A picture of the space of typical learnable tasks. *arXiv preprint arXiv:2210.17011*, 2022.
- [27] Yifei Lou, Andrei Irimia, Patricio A Vela, Micah C Chambers, John D Van Horn, Paul M Vespa, and Allen R Tannenbaum. Multimodal deformable registration of traumatic brain injury mr volumes via the bhattacharyya distance. *IEEE Transactions on Biomedical Engineering*, 60(9):2511–2520, 2013.
- [28] Rui Zhao, Jinming Song, Yufeng Yuan, Haifeng Hu, Yang Gao, Yi Wu, Zhongqian Sun, and Wei Yang. Maximum entropy population-based training for zero-shot human-ai coordination. In *Proceedings of the AAAI Conference on Artificial Intelligence*, volume 37, pages 6145–6153, 2023.
- [29] Kevin P Balanda and HL MacGillivray. Kurtosis: a critical review. *The American Statistician*, 42(2):111–119, 1988.
- [30] Mikayel Samvelyan, Tabish Rashid, Christian Schroeder De Witt, Gregory Farquhar, Nantas Nardelli, Tim GJ Rudner, Chia-Man Hung, Philip HS Torr, Jakob Foerster, and Shimon Whiteson. The starcraft multi-agent challenge. *arXiv preprint arXiv:1902.04043*, 2019.
- [31] Chao Li, Shaokang Dong, Shangdong Yang, Yujing Hu, Wenbin Li, and Yang Gao. Coordinating multi-agent reinforcement learning via dual collaborative constraints. *Neural Networks*, 182:106858, 2025.
- [32] Songchen Fu, Shaojing Zhao, Ta Li, and Yonghong Yan. Qtypemix: Enhancing multi-agent cooperative strategies through heterogeneous and homogeneous value decomposition. *Neural Networks*, 184:107093, 2025.
- [33] Zhiwei Xu, Yunpeng Bai, Bin Zhang, Dapeng Li, and Guoliang Fan. HAVEN: Hierarchical cooperative multi-agent reinforcement learning with dual coordination mechanism. In *Proceedings of the AAAI Conference on Artificial Intelligence*, volume 37, pages 11735–11743, 2023.
- [34] Pengyi Li, Jianye Hao, Hongyao Tang, Yan Zheng, and Xian Fu. RACE: improve multi-agent reinforcement learning with representation asymmetry and collaborative evolution. In *International Conference on Machine Learning*, pages 19490–19503. PMLR, 2023.
- [35] Anuj Mahajan, Tabish Rashid, Mikayel Samvelyan, and Shimon Whiteson. MAVEN: Multi-agent variational exploration. *Advances in neural information processing systems*, 32, 2019.
- [36] Wei-Fang Sun, Cheng-Kuang Lee, Simon See, and Chun-Yi Lee. A unified framework for factorizing distributional value functions for multi-agent reinforcement learning. *Journal of Machine Learning Research*, 24(220):1–32, 2023.
- [37] Stephen P Boyd and Lieven Vandenberghe. *Convex optimization*. Cambridge university press, 2004.

## A Algorithm

The full specifications of our approach are described in Algorithms 2& 1. The main training loop begins in algorithm 1. The learning parameters are initialized at the beginning of the algorithm and the training loop is executed iteratively for  $X$  episodes. Action selection is performed in algorithm 2. Note that our proposed exploration is executed when the excess kurtosis is positive, otherwise, a standard epsilon greedy selection is performed. The critics' loss function can be divided into two parts, the Bhattacharyya term which ensures diversity in the ensemble, and the critic loss, which utilizes the weighted  $Q_{tot}$  to reduce variance in the centralized critic. Note that both the critics and the actors are trained with a mix of offline and online data. The online data is sampled from a smaller buffer  $\mathcal{D}_{on}$  and  $|N_2| > |N_1|$ .

---

### Algorithm 1: SEMUS Algorithm

---

**Input:**  $L$  (num of episodes),  $X$  target update interval,  $T$  (episode length),  $K$  (num of agents)  
Initialize centralized mixing network  $Q_{tot}^\phi$ , for each agent  $i$ : ensemble critics  $\{Q^{\phi_{i,j}}\}_{j=1}^N$ , actor networks  $\{\pi_{\theta_i}\}_{i=1}^k$   
Initialize target centralized critic  $Q_{tot}^{\phi'} = Q_{tot}^\phi$ , target ensemble critics  $Q^{\phi'_{i,j}} = Q^{\phi_{i,j}}$   
Initialize on-policy replay buffer  $\mathcal{D}_{on}$ , off-policy replay buffer  $\mathcal{D}_{off}$   
**for** episode = 1 to  $L$  **do**  
  Initialize environment and agents  
  **for**  $t = 1$  to  $T$  **do**  
    Observe state  $s_t$   
    obtain joint action set  $\mathbf{a}_t$  by calling Algorithm 2  
    Execute joint actions  $\mathbf{a}_t$   
    Receive reward  $r_t$  and next state  $s_{t+1}$   
    Store transition  $(s_t, \mathbf{a}_t, r_t, s_{t+1})$  in replay buffers  $\mathcal{D}_{on}$  and  $\mathcal{D}_{off}$   
    Sample minibatch  $N_1$  from replay buffer  $\mathcal{D}_{on}$   
    Sample minibatch  $N_2$  from replay buffer  $\mathcal{D}_{off}$   
    Calculate the Bhattacharyya loss  $\delta_{B_{total}}^{Q_i}$  for sampled batches  $\{N_2, N_1\}$   
    Update the critics with the loss in Eq. 16 using a mix of on-policy and off-policy losses.  
    Update decentralized actors using a mix of on-policy and off-policy loss functions (Eq. 17)  
    **if**  $t \bmod X = 0$  **then**  
      Update target networks:  $Q^{\phi'_{i,j}} = Q^{\phi_{i,j}}$ ,  $Q_{tot}^{\phi'} = Q_{tot}^\phi$   
    **end if**  
  **end for**  
**end for**

---



---

### Algorithm 2: Action Selection

---

**Input:** actor policies  $\{\pi_i(a_i|\tau_i; \theta_i)\}_{i=1}^k$ , individual Q-functions  $\{Q_i^{\phi_i}\}_{i=1}^k$ , joint trajectory  $\tau$ , num\_agents, action space sizes  $\{M_i\}_{i=1}^k$   
**Output:** Selected actions set  $\mathbf{a}$   
**for** agent  $i = 1$  to num\_agents **do**  
  Get action logits  $\bar{z}^i = f_{\theta_i}(\tau_i)$   
  Calculate kurtosis over all actions for each agent:  

$$\bar{g}_i(\tau_i, \{Q^{\phi_{i,j}}\}_{j=1}^N) = \frac{\sum_{z=1}^{M_i} \kappa_{e, Q_i}^{\phi_i}(\tau_i, a_z)}{M_i},$$
  
  Update action logits according to Eq. 10 and the value of  $\bar{g}_i$   
  Select action  $a_i \sim \sigma(\bar{z}_j)$  with the updated logits using epsilon greedy policy.  
**end for**

---

## B Training Parameters and Computation Resources

Configurations and hyper-parameter values are provided in table 7. All experiments are conducted on stations with 64 Intel(R) Xeon(R) CPU E5-2683 v4 @ 2.10GHz, 251G RAM, and NVIDIA GeForce GTX 1080 Ti 12GB.

Table 7: Hyperparameter Table — SMAC

Hyperparameter	Value	Hyperparameter	Value
$T$ (train interval)	20K	$N_1$	32
$U$ (num test episodes)	24	$N_2$	5000
$C_1$	0.5	Ensemble size ( $N$ )	10
$C_2$	0.002		
$\beta$	0.004		
$v$	0.5		

## C Starcraft II Scenarios

Our main focus is on scenarios that require the agents to learn diverse skills or exhibit some level of exploration to solve the task. We use the term diversity to describe inter-agent diversification, meaning different agents acquiring different sets of skills.

**MMM2.** Two identical teams battle each other, aiming to eliminate the units of the opposing team. Each team controls 3 types of units: healer Medivac, attacking Marine units, and Marauders, capable of attacking enemy ground units. The MMM2 scenario requires diversity among agents, where each type of agent needs to learn a different set of strategies.

**MMM3 (7m2M1M vs 9m3M1M)**. This is an ultra hard version of the MMM2 map [36]. The allies control a smaller team of 10 agents compared to the larger enemy team of 13 agents.

**1c3s5z vs 1c3s6z.** A scenario where both teams control 3 types of agents, Colossus, Stalkers, and Zealots. The enemy team has a higher number of Zealots.

**3s vs 5z.** In this scenario, 3 Stalkers (ranged units) are controlled by agents facing 5 Zealots (melee units). The challenge lies in overcoming the numerical disadvantage by leveraging Stalkers’ kiting abilities, coordinating attacks.

## D Proof of Proposition 1

To prove Proposition 1, we measure the difference between the gradient of the true objective  $\nabla_{\theta_i} J(\pi_i, \pi_{-i})$  and the mixed gradient update  $D_{\nu}^{\beta} J(\pi_i, \pi_{-i})$ . Our technique is based on the proof presented in [13]. We conclude the appendix by outlining the key differences between their results and ours.

First, we simplify the on-policy term in Eq. 17:

$$\begin{aligned}
& \mathbb{E}_{\pi_i} [\nabla_{\theta_i} \log \pi_i(a_i | \tau_i) U_{\pi_i}^{\phi_i}(\tau_i, a_i)] \\
&= \mathbb{E}_{\pi_i} \left[ \nabla_{\theta_i} \log \pi_i(a_i | \tau_i) \lambda_i(\boldsymbol{\tau}) \left( Q_i^{\phi_i}(\tau_i, a_i) - \sum_x \pi_i(x | \tau_i) Q_i^{\phi_i}(\tau_i, x) \right) \right] \\
&= \mathbb{E}_{\pi_i} \left[ \nabla_{\theta_i} \log \pi_i(a_i | \tau_i) \lambda_i(\boldsymbol{\tau}) Q_i^{\phi_i}(\tau_i, a_i) \right], \tag{25}
\end{aligned}$$

and define the discounted joint state distribution as:

$$\rho^{\boldsymbol{\pi}}(\boldsymbol{\tau}) = \sum_{t=0}^{\infty} \gamma^t \rho_t^{\boldsymbol{\pi}}(\boldsymbol{\tau}), \tag{26}$$

where  $\rho_t^{\boldsymbol{\pi}}(\boldsymbol{\tau}) = p^{\boldsymbol{\pi}}(\tau_t = \boldsymbol{\tau})$  denotes the state distribution at time  $t$ , following a joint policy  $\boldsymbol{\pi}$ . Then, we can use the following lemma from [13]:

**Lemma 2.** Let  $\rho_t^{\boldsymbol{\pi}}$  and  $\rho_t^{\boldsymbol{\beta}}$  be two state distributions at time  $t$ . Then the following bound holds:

$$\|\rho_t^{\boldsymbol{\pi}} - \rho_t^{\boldsymbol{\beta}}\|_1 \leq 2t \sqrt{D_{\max}^{\text{KL}}(\boldsymbol{\pi}, \boldsymbol{\beta})}. \tag{27}$$

Given Lemma 2 we are ready to derive a bound on the left-hand side of Eq. 22:

$$\begin{aligned}
& \left\| \nabla_{\theta_i} J(\pi_i, \boldsymbol{\pi}_{-i}) - D_{\nu}^{\beta}(\pi_i, \boldsymbol{\pi}_{-i}) \right\|_1 \\
&= \left\| \mathbb{E}_{\rho^{\boldsymbol{\pi}}, \pi_i} \left[ \nabla_{\theta_i} \log \pi_i(a_i | \tau_i; \theta_i) Q_i^{\boldsymbol{\pi}}(\boldsymbol{\tau}, a_i) \right] \right. \\
&\quad \left. - (1 - \nu) \mathbb{E}_{\rho^{\boldsymbol{\pi}}, \pi_i} \left[ \nabla_{\theta_i} \log \pi_i(a_i | \tau_i; \theta_i) \lambda_i(\boldsymbol{\tau}) Q_i^{\phi_i}(\tau_i, a_i) \right] \right. \\
&\quad \left. - \nu \mathbb{E}_{\rho^{\beta}} \left[ \nabla_{\theta_i} \bar{Q}_{\text{tot}}^{\phi}(\boldsymbol{\tau}, (a_i, \mathbf{a}_{-i})) \right] \right\|_1 \\
&\stackrel{(*)}{=} \left\| \mathbb{E}_{\rho^{\boldsymbol{\pi}}, \pi_i} \left[ \nabla_{\theta_i} \log \pi_i(a_i | \tau_i; \theta_i) \left( Q_i^{\boldsymbol{\pi}}(\boldsymbol{\tau}, a_i) - \lambda_i(\boldsymbol{\tau}) Q_i^{\phi_i}(\tau_i, a_i) \right) \right] \right. \\
&\quad \left. + \nu \mathbb{E}_{\rho^{\boldsymbol{\pi}}, \pi_i} \left[ \nabla_{\theta_i} \log \pi_i(a_i | \tau_i; \theta_i) \lambda_i(\boldsymbol{\tau}) Q_i^{\phi_i}(\tau_i, a_i) \right] \right. \\
&\quad \left. - \nu \mathbb{E}_{\rho^{\beta}} \left[ \nabla_{\theta_i} \lambda_i(\boldsymbol{\tau}) \mathbb{E}_{\pi_i} [Q_i^{\phi_i}(\tau_i, a_i)] \right] \right\|_1 \\
&\stackrel{(**)}{\leq} \left\| \mathbb{E}_{\rho^{\boldsymbol{\pi}}, \pi_i} \left[ \nabla_{\theta_i} \log \pi_i(a_i | \tau_i; \theta_i) \left( Q_i^{\boldsymbol{\pi}}(\boldsymbol{\tau}, a_i) - \lambda_i(\boldsymbol{\tau}) Q_i^{\phi_i}(\tau_i, a_i) \right) \right] \right\|_1 \\
&\quad \left. + \nu \left\| \mathbb{E}_{\rho^{\boldsymbol{\pi}}, \pi_i} \left[ \nabla_{\theta_i} \log \pi_i(a_i | \tau_i; \theta_i) \lambda_i(\boldsymbol{\tau}) Q_i^{\phi_i}(\tau_i, a_i) \right] \right. \right. \\
&\quad \left. \left. - \mathbb{E}_{\rho^{\beta}} \left[ \nabla_{\theta_i} \lambda_i(\boldsymbol{\tau}) \mathbb{E}_{\pi_i} [Q_i^{\phi_i}(\tau_i, a_i)] \right] \right\|_1 \right. \\
&\stackrel{(***)}{\leq} \omega_1 \sum_{t=0}^{\infty} \gamma^t + \nu \omega_2 \sum_{t=0}^{\infty} \gamma^t \left\| \rho_t^{\boldsymbol{\pi}} - \rho_t^{\beta} \right\|_1 \\
&\leq \frac{\omega_1}{1 - \gamma} + 2\nu \omega_2 \left( \sum_{t=0}^{\infty} \gamma^t t \right) \sqrt{D_{\max}^{\text{KL}}(\boldsymbol{\pi}, \boldsymbol{\beta})} \\
&= \frac{\omega_1}{1 - \gamma} + \frac{2\omega_2 \nu \gamma}{(1 - \gamma)^2} \sqrt{D_{\max}^{\text{KL}}(\boldsymbol{\pi}, \boldsymbol{\beta})}. \tag{29}
\end{aligned}$$

Equality  $(*)$  leverages the additive structure of  $Q_{\text{tot}}$  by replacing

$Q_{\text{tot}}^{\phi}(\boldsymbol{\tau}, (a_i, \mathbf{a}_{-i}))$  with  $Q_i^{\phi_i}(\boldsymbol{\tau}, a_i)$ , this is allowed since applying the gradient with respect to  $\theta_i$  cancels out all the components of  $Q_{\text{tot}}$  that are independent of  $Q_i$ . Inequality  $(**)$  rearranges the terms and utilizes the triangle inequality to separate the original term into 2 different expressions. In inequality  $(***)$  and onward, we bound the bias by taking the maximum value of each expression and extracting  $\omega_1$  and  $\omega_2$  from the respective sums. The first term is bounded with  $\omega_1$  as follows:

$$\begin{aligned}
& \left\| \mathbb{E}_{\rho^{\boldsymbol{\pi}}, \pi_i} \left[ \nabla_{\theta_i} \log \pi_i(a_i | \tau_i; \theta_i) \left( Q_i^{\boldsymbol{\pi}}(\boldsymbol{\tau}, a_i) - \lambda_i(\boldsymbol{\tau}) Q_i^{\phi_i}(\tau_i, a_i) \right) \right] \right\|_1 \\
&= \left\| \sum_{t=0}^{\infty} \gamma^t \sum_{\boldsymbol{\tau}} \rho_t^{\boldsymbol{\pi}}(\boldsymbol{\tau}) \sum_{a_i \in \mathcal{A}} \pi_i(a_i | \tau_i; \theta_i) \nabla_{\theta_i} \log \pi_i(a_i | \tau_i; \theta_i) \right. \\
&\quad \left. \left( Q_i^{\boldsymbol{\pi}}(\boldsymbol{\tau}, a_i) - \lambda_i(\boldsymbol{\tau}) Q_i^{\phi_i}(\tau_i, a_i) \right) \right\|_1 \\
&\leq \max_{\boldsymbol{\tau}, \mathbf{a}} \left\| \nabla_{\theta_i} \log(\pi_i(a_i | \tau_i; \theta_i)) \lambda_i(\boldsymbol{\tau}) Q_{\phi_i}^{\boldsymbol{\pi}}(\boldsymbol{\tau}, a_i) \right\|_1 \sum_{t=0}^{\infty} \gamma^t \sum_{\boldsymbol{\tau}} \rho_t^{\boldsymbol{\pi}}(\boldsymbol{\tau}), \tag{30}
\end{aligned}$$

with  $\sum_{\boldsymbol{\tau}} \rho_t^{\boldsymbol{\pi}}(\boldsymbol{\tau}) = 1$  and  $\omega_1$  equal the maximum over  $\boldsymbol{\tau}$  and  $\mathbf{a}$ . The second term, which we bound using  $\omega_2$ , represents the difference between two distinct mean expressions. To derive a bound, we need to ensure that the same expression appears inside both means. Using the following equality:

$$\nabla_{\theta_i} \log \pi_i(a_i | \tau_i; \theta_i) = \frac{\nabla_{\theta_i} \pi_i(a_i | \tau_i; \theta_i)}{\pi_i(a_i | \tau_i; \theta_i)}, \tag{31}$$

we can write:

$$\begin{aligned}
& \mathbb{E}_{\rho^\pi, \pi_i} \left[ \nabla_{\theta_i} \log \pi_i(a_i | \tau_i; \theta_i) \lambda_i(\boldsymbol{\tau}) Q_i^{\phi_i}(\tau_i, a_i) \right] \\
&= \mathbb{E}_{\rho^\pi, \pi_i} \left[ \frac{\nabla_{\theta_i} \pi_i(a_i | \tau_i; \theta_i)}{\pi_i(a_i | \tau_i; \theta_i)} \lambda_i(\boldsymbol{\tau}) Q_i^{\phi_i}(\tau_i, a_i) \right] \\
&= \mathbb{E}_{\rho^\pi} \left[ \sum_{a_i \in \mathcal{A}} \pi_i(a_i | \tau_i; \theta_i) \frac{\nabla_{\theta_i} \pi_i(a_i | \tau_i; \theta_i)}{\pi_i(a_i | \tau_i; \theta_i)} \lambda_i(\boldsymbol{\tau}) Q_i^{\phi_i}(\tau_i, a_i) \right] \\
&= \mathbb{E}_{\rho^\pi} \left[ \nabla_{\theta_i} \lambda_i(\boldsymbol{\tau}) \mathbb{E}_{\pi_i} [Q_i^{\phi_i}(\tau_i, a_i)] \right], \tag{32}
\end{aligned}$$

and apply it to the second term:

$$\begin{aligned}
& \left\| \mathbb{E}_{\rho^\pi} \left[ \nabla_{\theta_i} \lambda_i(\boldsymbol{\tau}) \mathbb{E}_{\pi_i} [Q_i^{\phi_i}(\tau_i, a_i)] \right] - \mathbb{E}_{\rho^\beta} \left[ \nabla_{\theta_i} \lambda_i(\boldsymbol{\tau}) \mathbb{E}_{\pi_i} [Q_i^{\phi_i}(\tau_i, a_i)] \right] \right\|_1 \\
&\leq \sum_{t=0}^{\infty} \gamma^t \left\| \mathbb{E}_{\rho_t^\pi} \left[ \nabla_{\theta_i} \lambda_i(\boldsymbol{\tau}) \mathbb{E}_{\pi_i} [Q_i^{\phi_i}(\tau_i, a_i)] \right] - \mathbb{E}_{\rho_t^\beta} \left[ \nabla_{\theta_i} \lambda_i(\boldsymbol{\tau}) \mathbb{E}_{\pi_i} [Q_i^{\phi_i}(\tau_i, a_i)] \right] \right\|_1 \\
&\leq \max_{\boldsymbol{\tau}} \left\| \nabla_{\theta_i} \lambda_i(\boldsymbol{\tau}) \mathbb{E}_{\pi_i} [Q_i^{\phi_i}(\tau_i, a_i)] \right\|_1 \sum_{t=0}^{\infty} \gamma^t \left\| \rho_t^\pi - \rho_t^\beta \right\|_1. \tag{33}
\end{aligned}$$

□

Note that the original work on mixed samples actor in the single agent-domain also formed a bound on the bias. There are several differences between our proof and [13]: (1) They bounded the objective  $J$  while we bound the gradient of the objective ( $\nabla J$ ). Bounding the gradients is usually associated with additional aspects other than optimality and errors in  $J$ , such as stability and variance (how noisy the updates are, for instance [2]), those are extremely important in multi-agent settings, as agents may destabilize the learning process of one another during training. (2) As The main goal in adapting the bound to multi-agent settings was to assess the effect agents have on the bias of one another. It required a different construction of  $Q_i^\pi$  and the true objective's gradient  $\nabla J(\pi_i, \pi^{-i})$ , since both terms have to be estimated via  $Q_{tot}$  and account for all agents.

## E Proof of Proposition 2.

In this subsection, we show that applying the Bhattacharyya regularization between the mean Q-function in the ensemble and each other member (as suggested in the main paper) yields a lower bound on a pairwise Bhattacharyya regularization. This reduces the computation requirements, from  $\mathcal{O}(N^2)$  operations of the pairwise approach to  $\mathcal{O}(N)$  calculations that the mean approach requires.

In the main paper, we defined the Bhattacharyya term for a single ensemble as:

$$\delta_{B_{total}}^{Q_i}(\tau_i) = \sum_{j=1}^N \delta_B \left( \sigma \left( Q_i^{\phi_i}(\tau_i, \cdot) \right), \sigma \left( Q^{\phi_{i,j}}(\tau_i, \cdot) \right) \right), \tag{34}$$

where  $Q_i^{\phi_i}$  is the mean Q-value in the ensemble, and  $Q^{\phi_{i,j}}$  denotes the individual Q-function of the  $j_{th}$  member within the ensemble. For ease of notation, we define:

$$\delta_{mean}^i = \frac{\delta_{B_{total}}^{Q_i}(\tau_i)}{N}, \quad P_i = \sigma \left( Q_i^{\phi_i}(\tau_i, \cdot) \right), \quad P_{i,j} = \sigma \left( Q^{\phi_{i,j}}(\tau_i, \cdot) \right), \tag{35}$$

The average pairwise Bhattacharyya distance is defined as:

$$\delta_{pairwise}^i = \frac{1}{N^2} \sum_{j_1=1}^N \sum_{j_2=1}^N \delta_B \left( \sigma \left( Q^{\phi_{i,j_1}}(\tau_i, \cdot) \right), \sigma \left( Q^{\phi_{i,j_2}}(\tau_i, \cdot) \right) \right). \tag{36}$$

**Proposition 3 .** Let the Bhattacharyya distance between the mean and each member be denoted by  $\delta_{mean}^i$  and the pairwise Bhattacharyya distance denoted by  $\delta_{pairwise}^i$ , then the following holds:

$$\delta_{mean}^i \leq \delta_{pairwise}^i. \tag{37}$$

**Proof .** We begin by defining the Bhattacharyya coefficient:

$$BC(P_i, P_{i,j}) := \sum_{a \in \mathcal{A}} \sqrt{P_i(a)P_{i,j}(a)}, \quad (38)$$

where the Bhattacharyya distance between  $P_i$  and  $P_{i,j}$  is defined as:  $\delta_B(P_i, P_{i,j}) = -\ln(BC(P_i, P_{i,j}))$ . For each member  $P_{i,j}$  in the ensemble, we use the concavity of the Bhattacharyya coefficient in each of its arguments, and obtain the following inequality between the mean-based and the pairwise coefficients:

$$BC(P_{i,j}, P_i) \geq \frac{1}{N} \sum_{j'=1}^N BC(P_{i,j}, P_{i,j'}), \quad (39)$$

which stems from the definition of  $P_i$  and the concavity of the geometric mean [37]:

$$\begin{aligned} BC(P_{i,j}, P_i) &= \sum_a \sqrt{P_{i,j}(a) \left( \frac{1}{N} \sum_{j'=1}^N P_{i,j'}(a) \right)} \\ &\geq \frac{1}{N} \sum_{j'=1}^N \sum_a \sqrt{P_{i,j}(a)P_{i,j'}(a)} \\ &= \frac{1}{N} \sum_{j'=1}^N BC(P_{i,j}, P_{i,j'}). \end{aligned} \quad (40)$$

Next, we apply  $-\ln(x)$  on both sides:

$$-\ln(BC(P_{i,j}, P_i)) \leq -\ln\left(\frac{1}{N} \sum_{j'=1}^N BC(P_{i,j}, P_{i,j'})\right), \quad (41)$$

and use the convexity of  $-\ln(x)$  on the expression on the right side of the inequality, we get:

$$-\ln\left(\frac{1}{N} \sum_{j'=1}^N BC(P_{i,j}, P_{i,j'})\right) \leq \frac{-\ln(\sum_{j'=1}^N BC(P_{i,j}, P_{i,j'}))}{N}. \quad (42)$$

Combining equations 41-42 and summing over  $j$  (all members in the ensemble) gives us:

$$\sum_{j=1}^N -\ln(BC(P_{i,j}, P_i)) \leq \frac{\sum_{j_1=1}^N -\ln(\sum_{j_2=1}^N BC(P_{i,j_1}, P_{i,j_2}))}{N}. \quad (43)$$

Dividing both sides by  $N$  yields Eq. 37. □

## F Proof of Lemma 1

we examine a controlled model where each critic satisfies  $Q^{\phi_{i,j}} = \mu + \delta_j$ , with  $\delta_j \in \{0, \Delta\}$ ,  $P(\delta_j = \Delta) = p_j$ , and  $\bar{p} = \frac{1}{N} \sum_j p_j$ . Under the assumption that  $\Delta$  is shared, kurtosis depends only on the disagreement probability  $\bar{p}$  and not on magnitude.

**Lemma 1.** For every  $\Delta > 0$ ,  $\text{Var}[\{Q^{\phi_{i,j}}\}_{j=1}^N] = \bar{p}(1-\bar{p})\Delta^2$ , whereas  $\kappa(\{Q^{\phi_{i,j}}\}_{j=1}^N) = \frac{1-6\bar{p}(1-\bar{p})}{\bar{p}(1-\bar{p})}$ .

**Proof.** Fix any  $(\tau_i, a_i)$  and write  $Q^{\phi_{i,j}}(\tau_i, a_i) = \mu + \delta_j$  for, where  $\mu = \mu(\tau_i, a_i)$ .

Since  $\mathbb{E}[\delta_j] = p_j\Delta$  and  $\frac{1}{N} \sum_j p_j = \bar{p}$ , the population mean of the ensemble distribution is:

$$\mu^* = \mathbb{E}[Q^{\phi_{i,j}}] = \mu + \bar{p}\Delta. \quad (44)$$

For each  $j$ , the deviation from  $\mu^*$  is:

$$Q^{\phi_{i,j}} - \mu^* = \begin{cases} -\bar{p}\Delta & \text{with probability } 1 - p_j, \\ (1 - \bar{p})\Delta & \text{with probability } p_j. \end{cases} \quad (45)$$

Because  $\mu$  is common to all members there are no member-specific offsets to track; the deviations in (45) depend on  $j$  only through  $p_j$ .

Population variance:

$$\begin{aligned}
\text{Var} &= \frac{1}{N} \sum_{j=1}^N \mathbb{E}_{\delta_j} \left[ (Q^{\phi_{i,j}} - \mu^*)^2 \right] \\
&= \frac{1}{N} \sum_{j=1}^N [(1-p_j) \bar{p}^2 \Delta^2 + p_j (1-\bar{p})^2 \Delta^2] \\
&= \Delta^2 [\bar{p}^2 + \bar{p}((1-\bar{p})^2 - \bar{p}^2)] \\
&= \bar{p}(1-\bar{p}) \Delta^2,
\end{aligned} \tag{46}$$

where we used  $\frac{1}{N} \sum_j p_j = \bar{p}$  and  $(1-\bar{p})^2 - \bar{p}^2 = 1 - 2\bar{p}$ .

Population fourth central moment:

$$\begin{aligned}
\hat{\mu}_4 &= \frac{1}{N} \sum_{j=1}^N \mathbb{E}_{\delta_j} \left[ (Q^{\phi_{i,j}} - \mu^*)^4 \right] \\
&= \frac{1}{N} \sum_{j=1}^N [(1-p_j) \bar{p}^4 \Delta^4 + p_j (1-\bar{p})^4 \Delta^4] \\
&= \bar{p}(1-\bar{p}) \Delta^4 [\bar{p}^3 + (1-\bar{p})^3].
\end{aligned} \tag{47}$$

Applying the identity  $\bar{p}^3 + (1-\bar{p})^3 = 1 - 3\bar{p}(1-\bar{p})$ :

$$\hat{\mu}_4 = \bar{p}(1-\bar{p}) [1 - 3\bar{p}(1-\bar{p})] \Delta^4. \tag{48}$$

Population excess kurtosis:

$$\begin{aligned}
\kappa(\{Q^{\phi_{i,j}}\}_{j=1}^N) - 3 &= \frac{\hat{\mu}_4}{\text{Var}^2} - 3 \\
&= \frac{\bar{p}(1-\bar{p}) [1 - 3\bar{p}(1-\bar{p})] \Delta^4}{\bar{p}^2 (1-\bar{p})^2 \Delta^4} - 3 \\
&= \frac{1 - 3\bar{p}(1-\bar{p})}{\bar{p}(1-\bar{p})} - 3 \\
&= \frac{1 - 6\bar{p}(1-\bar{p})}{\bar{p}(1-\bar{p})}.
\end{aligned} \tag{49}$$

□